

Exceptional service in the national interest



Materials Compatibility in Dish-Stirling Solar Generators Using Cu-Mg-Si Eutectic for Latent Heat Storage

Elizabeth Withey, Alan Kruizenga, and Charles Andraka

Abstract

Dish-Stirling systems have a strong potential of meeting SunShot cost goals of 6¢/kWh. We are investigating a Cu-Mg-Si eutectic alloy, a metallic phase change material (PCM), for latent heat storage for increased capacity factor and constant temperature power delivery. The metallic alloy PCM is favored because of its high thermal conductivity, high heat of melting, and melting temperature match to the engine operating range. Here we attempt to mitigate the compatibility issues between Haynes 230 alloy containment vessel and Cu-Si-Mg eutectic alloy through the use of ceramic coatings, including Al_2O_3 , Y_2O_3 , and 20% Y_2O_3 -stabilized ZrO_2 (YSZ). Counter to thermodynamic reasoning, Haynes 230 was well protected by Al_2O_3 , while Y_2O_3 and YSZ coatings were severely attacked by the Cu-Mg-Si alloy.

Introduction

Containment of liquid metal phase change materials (PCMs) is a necessity for adding thermal energy storage (TES) to dish-Stirling concentrated power systems. With this addition, these systems stand to become cost competitive with conventional forms of energy production. However, materials compatibility issues arise when liquid metals come into contact other metallic alloys facilitating the need for protective coatings on containment vessels.

Materials

Cu-21.1Mg-25.3Si (wt.%) has been shown as a good candidate for TES due to its melting temperature match with the operating range of Stirling engines, high heat of melting, and high thermal conductivity. Haynes 230, Ni-Cr-W superalloy, was chosen for containment because it is already been proven effective in heat pipe technology used for heat transport in dish-Stirling systems. Expected challenges with this combination include:

1. High reactivity of Si with Ni and Cr
2. Complete miscibility of Ni and Cu
3. Volatility of Mg at elevated temperature

Three plasma sprayed coatings were chosen to mitigate these issues

1. 20wt.% Y_2O_3 -stabilized ZrO_2 (YSZ) (thermal stability)
2. Y_2O_3 (thermodynamic stability)
3. Al_2O_3 (known to contain liquid Si)

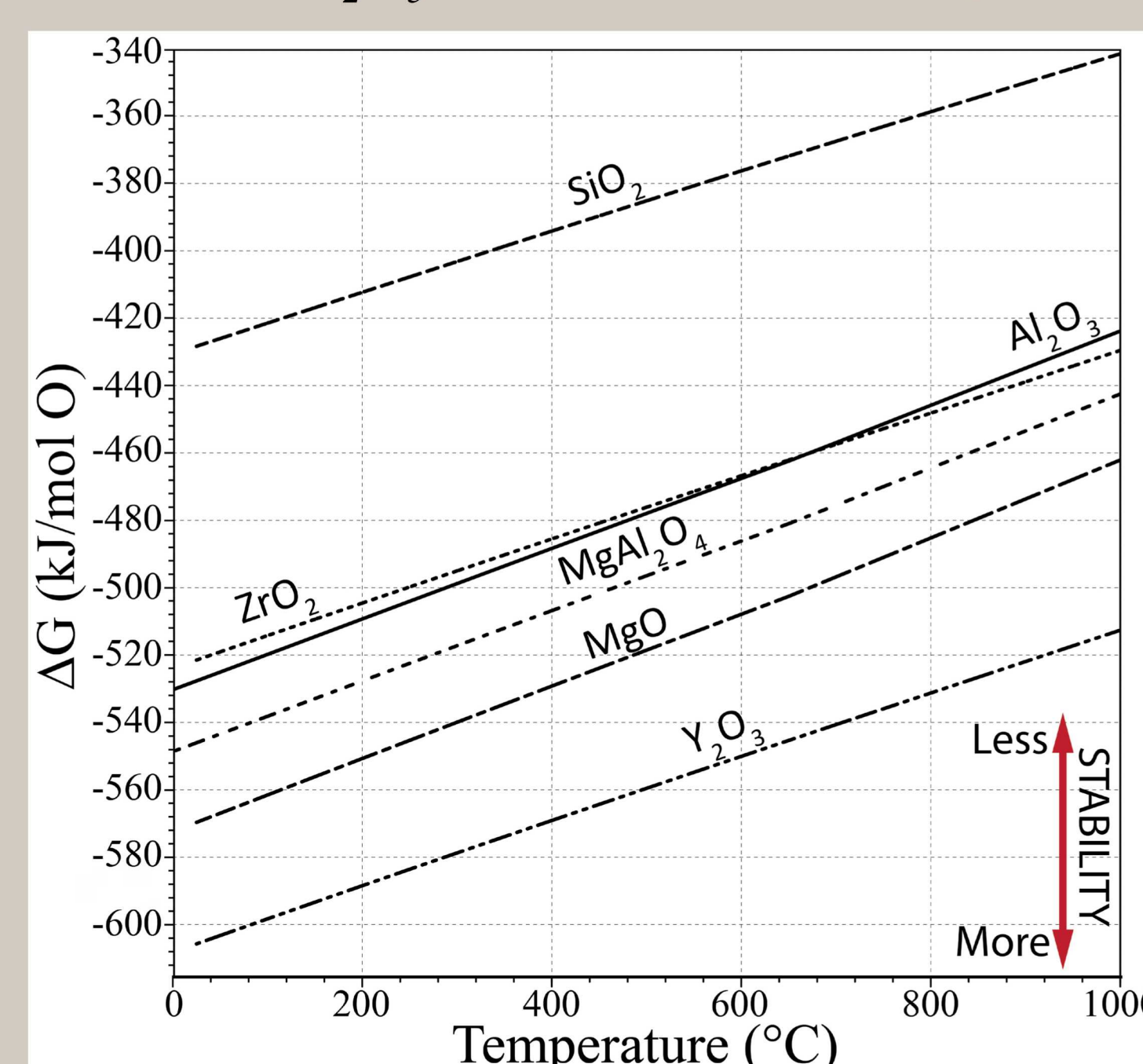


Figure 1: Ellingham diagram illustrating the relative stability of the protective coatings investigated compared to the oxides most likely to form from the PCM

Method

Haynes 230 boats, coated and uncoated, were filled with PCM, encapsulated in Ar atmosphere, and heated to 820 °C for 500 hours. boats were then potted and sectioned for microscopy and elemental mapping.

Results: Haynes 230

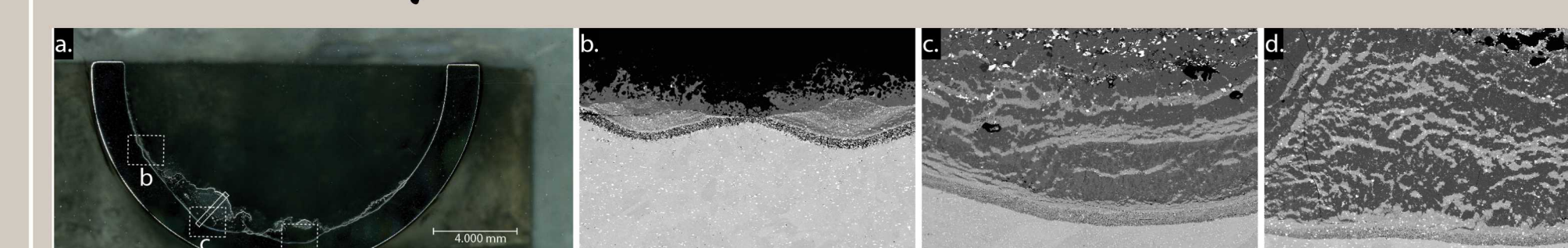


Figure 3: a) Optical micrograph of uncoated Haynes 230 boat exposed to PCM for 150 hrs at 820 °C, followed by SEM micrographs of the areas marked in (a).

Expected: Severe attack where Haynes 230 in contact with PCM

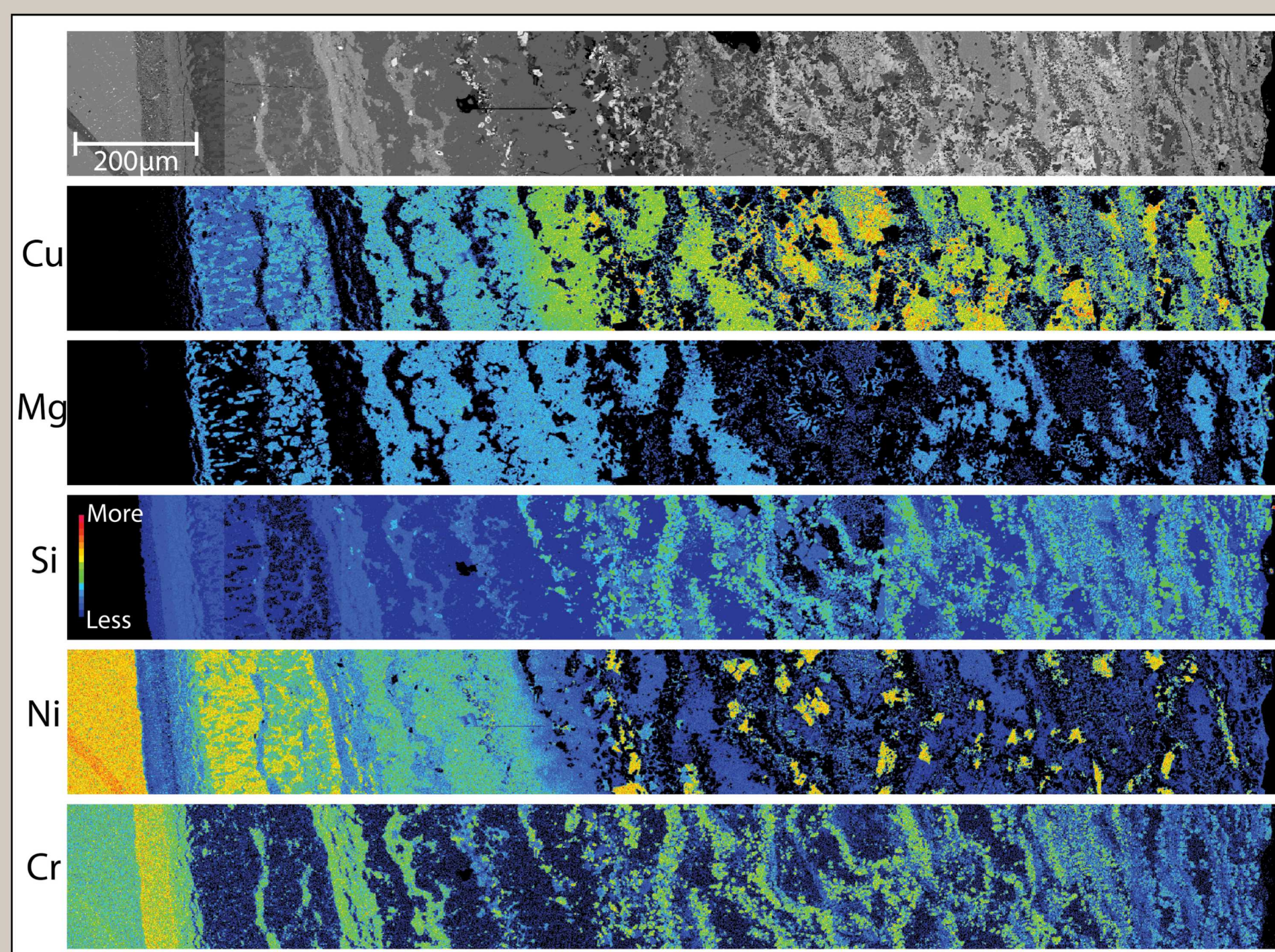


Figure 4: Elemental maps from electron microprobe analysis (EMPA) using wavelength dispersive spectroscopy (WDS) showing the relative amounts of relevant species after exposure to PCM. Haynes boat is at the left edge of the maps.

- Porous diffusion layer at edge of attack rich in Si and Cr and depleted of Ni
- Cu and Mg remain in PCM while Si attacks Haynes 230
- Ni and Cr diffuse into PCM overlapping with areas high in Si

Conclusions:

1. Haynes 230 is vigorously attacked when exposed to Si, which forms various silicides with Ni and Cr
2. 20% Y_2O_3 -stabilized ZrO_2 and Y_2O_3 plasma sprayed coatings do not adequately protect Haynes 230
3. Al_2O_3 plasma-sprayed coatings protect Haynes 230 from PCM, by reacting with Mg. Further testing is required to determine exact reaction
$$3\text{Mg} + \text{Al}_2\text{O}_3 \leftrightarrow 3\text{MgO} + 2\text{Al}$$

$$\text{MgO} + \text{Al}_2\text{O}_3 \leftrightarrow \text{MgAl}_2\text{O}_4$$

$$3\text{Mg} + 4\text{Al}_2\text{O}_3 \leftrightarrow 3\text{MgAl}_2\text{O}_4 + 2\text{Al}$$
4. MgAl_2O_4 is a good candidate for a protective coating on Haynes 230 for this application.

As Coated Coupons

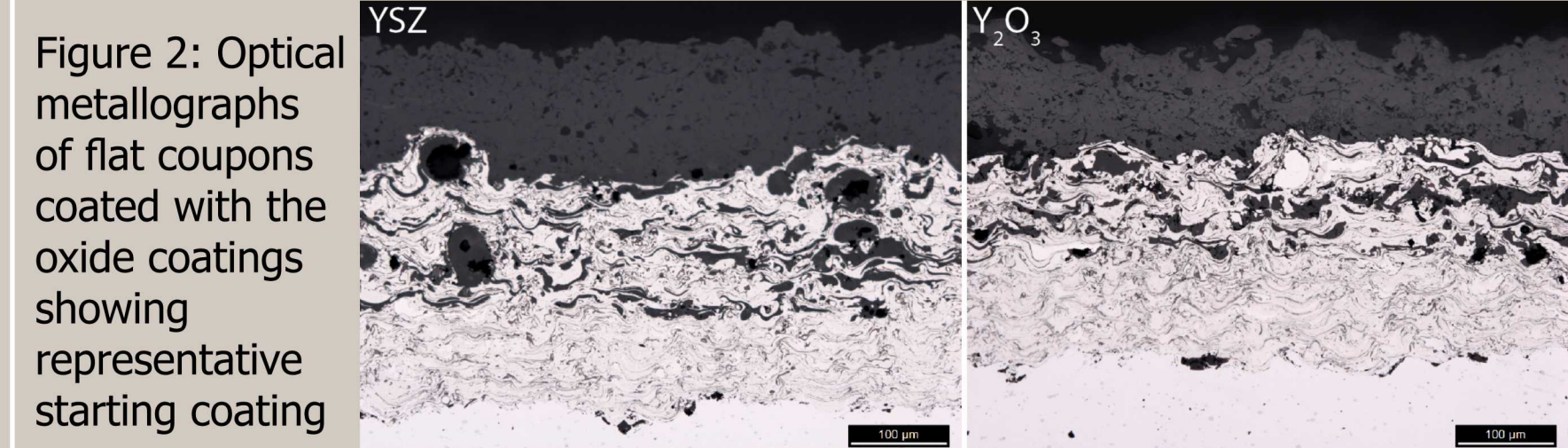


Figure 2: Optical metallographs of flat coupons coated with the oxide coatings showing representative starting coating

Oxide Coating (100-200 μm)
Transition: Oxide-Ni/Cr (100 μm)
Bond Layer: 80-20 Ni/Cr (100 μm)
Haynes 230 (1.5 mm)

Results: Al_2O_3 Coating

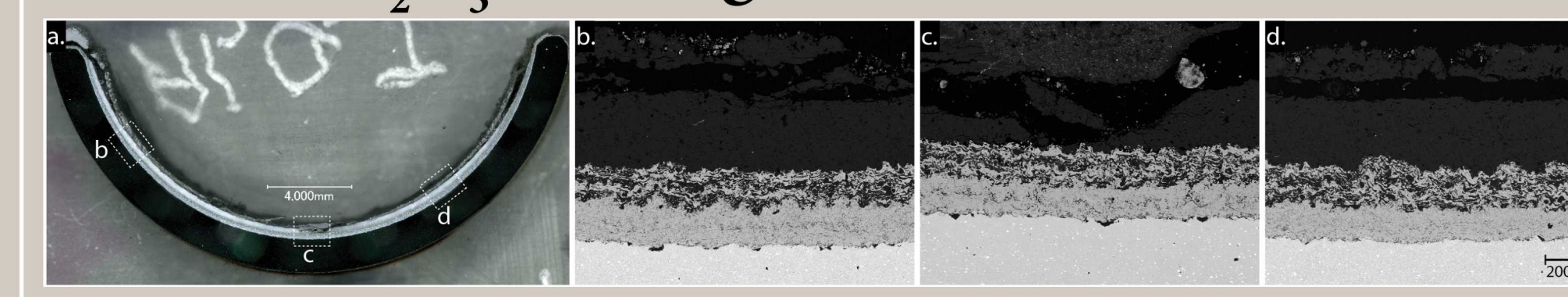


Figure 5: Optical overview and SEM images of corresponding areas of attack for the Al_2O_3 -coated boats,

Unexpected: Al_2O_3 not attacked by PCM*

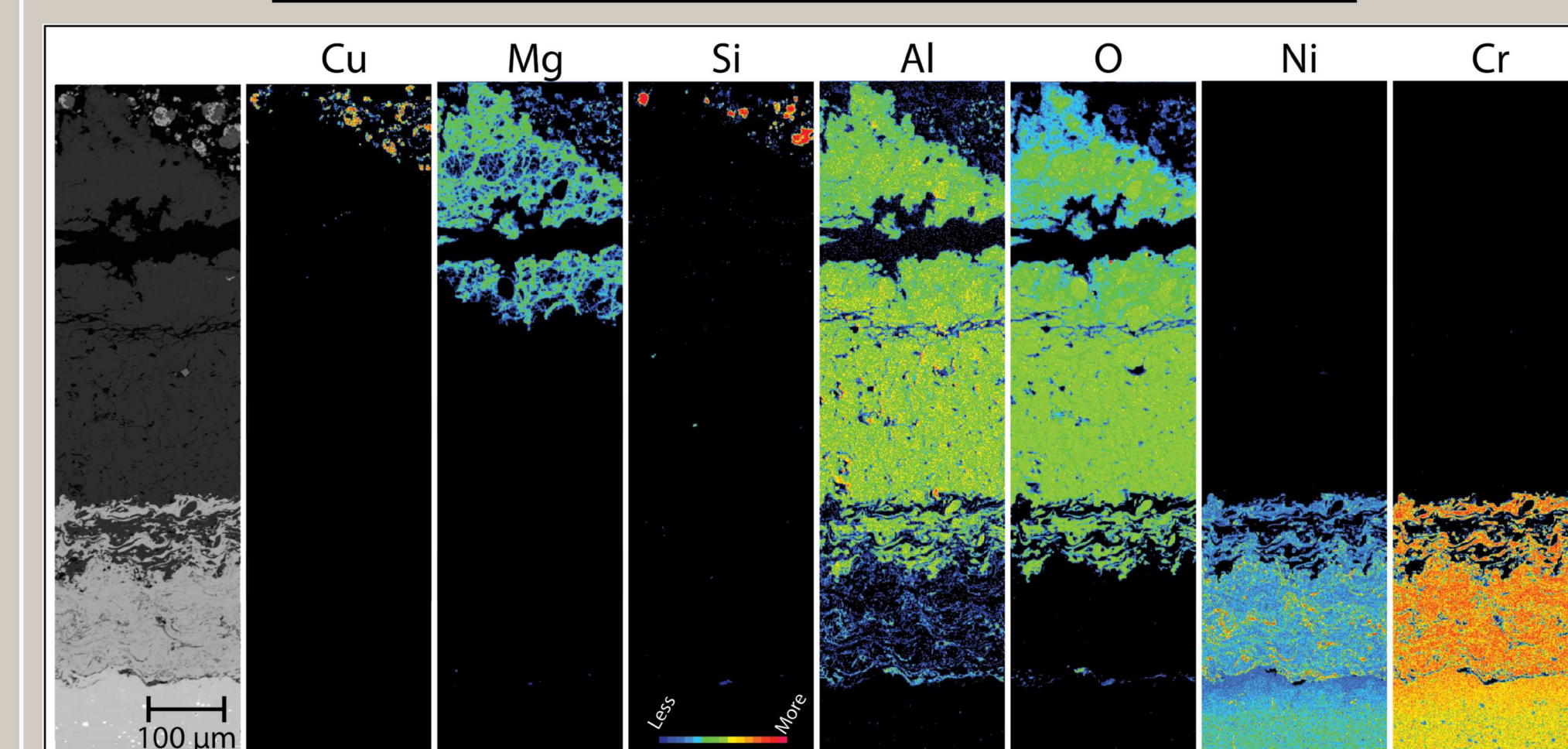


Figure 6: EMPA maps showing the relative amounts of relevant species after exposure of the Al_2O_3 -coated boat to PCM. Coating and PCM are at the top, Haynes 230 at bottom

- No Si or Cu past coating
- Mg overlaps with Al and O maps likely indicating mixture of MgO and MgAl_2O_4 through
$$3\text{Mg} + \text{Al}_2\text{O}_3 \leftrightarrow 3\text{MgO} + 2\text{Al}$$

$$\text{MgO} + \text{Al}_2\text{O}_3 \leftrightarrow \text{MgAl}_2\text{O}_4$$

$$3\text{Mg} + 4\text{Al}_2\text{O}_3 \leftrightarrow 3\text{MgAl}_2\text{O}_4 + 2\text{Al}$$

Results: YSZ and Y_2O_3 Coatings

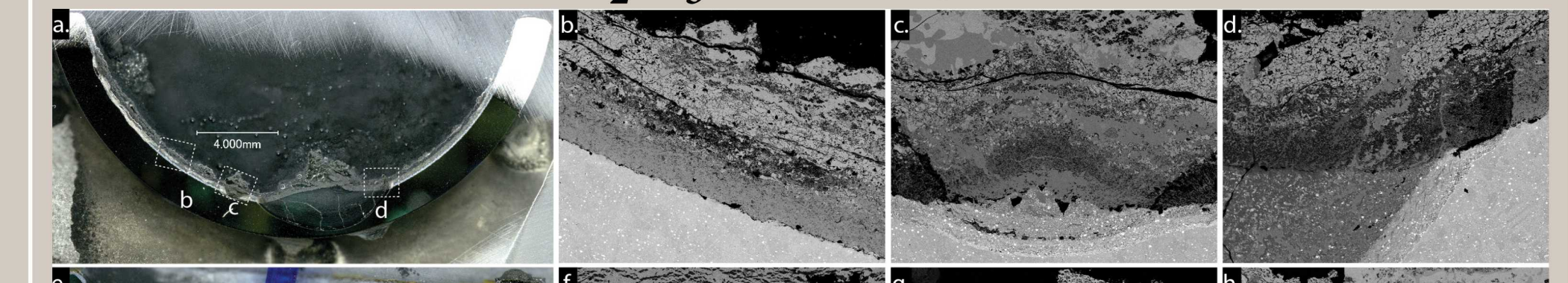
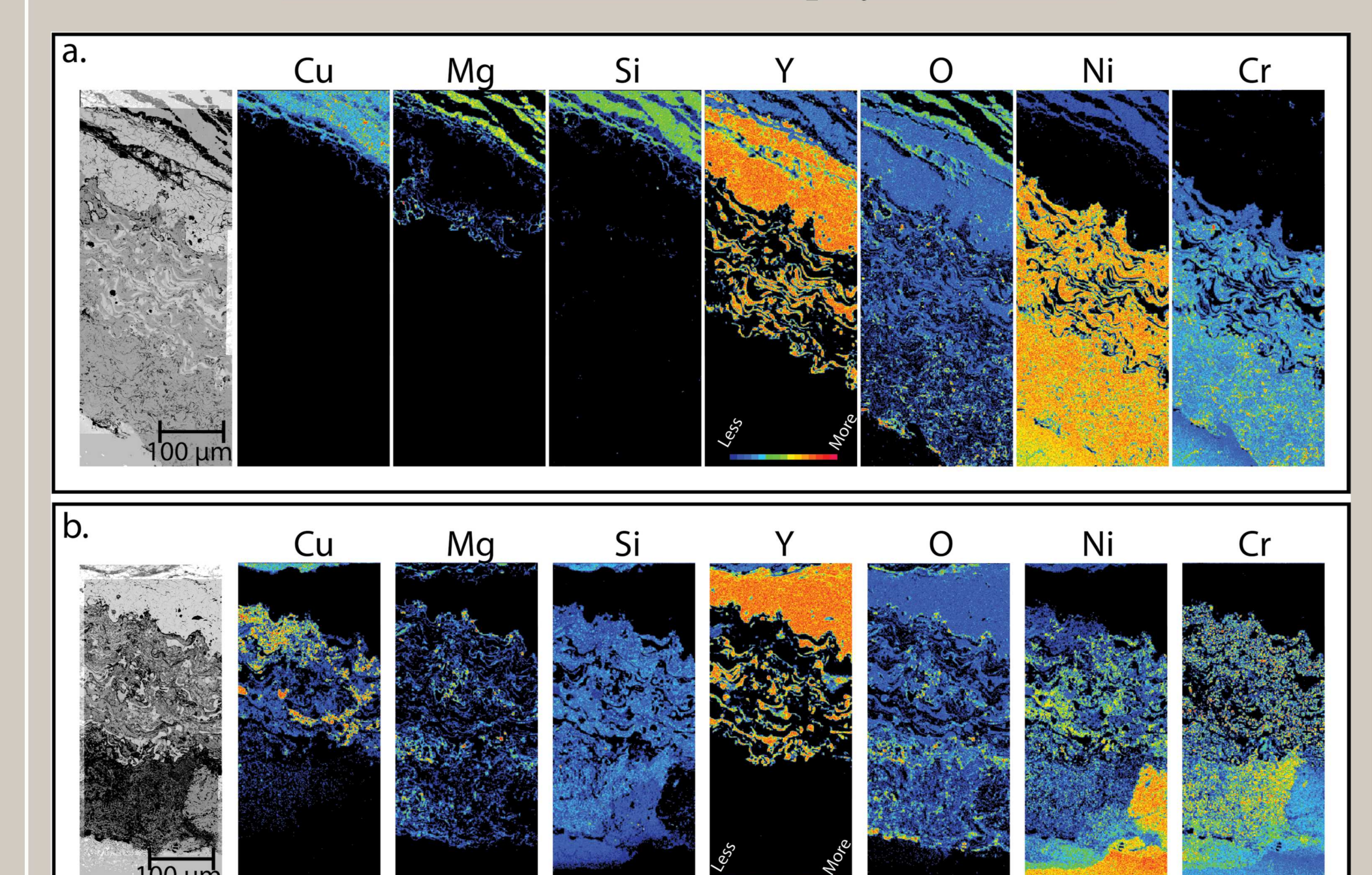


Figure 7: (a-d) and (e-h) optical overview and SEM images of corresponding areas of attack for the YSZ and Y_2O_3 -coated boats, respectively showing a wide range of attack depths.

Expected: Attack of YSZ coating*

Unexpected: Attack of Y_2O_3 coating*



- Mg infiltrated Yttria coating prior to Si or Cu
$$3\text{Mg} + \text{Y}_2\text{O}_3 \leftrightarrow 3\text{MgO} + 2\text{Y}$$
 (volume loss)
- Reaction leaves easy pathway for diffusion of Si
- Si follows Mg, Cu follows Si.
- Once Si reaches Haynes 230 interface, Si, Cr, and Ni diffuse quickly at temperature